# Polyelectrolyte/Surfactant Interaction: An NMR Characterization

**N. Proietti,*,† M. E. Amato,‡ G. Masci,§ and A. L. Segre†**

*Istituto di Metodologie Chimiche, CNR, Via Salaria km 29.300, 00016 Monterotondo Stazione, Roma, Italy; Dipartimento di Scienze Chimiche, Università degli Studi di Catania, Viale Andrea Doria 6, 95125 Catania, Italy; and Dipartimento di Chimica, Università degli Studi di Roma "La Sapienza", Piazzale Aldo Moro 5, 00185 Roma, Italy*

*Received December 26, 2001*

ABSTRACT: Interaction between a cationic copolymer (acrylamide−trimethylaminoethyl acrylate) P(AAm−TMA) and an anionic perfluorinated surfactant (lithium perfluorooctanoate) (LiPFO) was studied using $^{1}H$ and $^{19}F$ NMR. To clarify the effect of the charge density, copolymers having a different composition of comonomers have been used. In each copolymer−surfactant system the presence of the polyelectrolyte in solution strongly modifies the $^{19}F$ chemical shifts. Consequently, a strong polymer−surfactant interaction is evidenced. A complete saturation of the cationic charges of the polymer is clearly detectable, followed by a partial precipitation and subsequent redissolution of the system. The chemical shifts and line widths observed have been interpreted as dependent on two main factors: the aggregation state of the system and the rate of exchange among different sites. $^{1}H$ spectra, which run at a constant concentration of polymer and different concentrations of surfactant, appear rather broad and poorly defined. The spectral broadening becomes extremely marked at certain value *C* of the surfactant concentration, where a strong super-Lorentzian line appears, surmounted by weak sharp lines in which the chemical shift is still visible. Increasing the charge density the critical concentration *C* increases. A further increase in the surfactant concentration causes a sharp precipitation which is accompanied by the disappearance of the super-Lorentzian resonance. This critical concentration value *C* may be interpreted as being due to the so-called "cac", i.e., the concentration of critical aggregation. At a higher surfactant concentration, after the resolubilization, a super-Lorentzian $^{19}F$ line is observed superimposed again by a sharp spectrum. The presence of the super-Lorentzian $^{19}F$ line can be interpreted as an indicator of the incoming gelification of the mixture. A model of interaction has been proposed on the basis of the results obtained.

## Introduction

Flocculation of colloidal particles due to the introduction of a charged polymer into a liquid suspension is an important solid−liquid separation process in various industrial mineral processing and in municipal water and wastewater treatment.[1−5] In fact, adsorption of polyelectrolytes at the particle/liquid interface has a deep effect on the flocculation and the stabilization behavior of colloidal suspensions. At low surfactant doses flocculation can occur, while at high surfactant doses the suspension can be resolubilized. Very long and extended charged macromolecules can become adsorbed on more than one charged particle producing a bridging mechanism,[6] resulting in a marked flocculation of the entire system.

Negatively charged kaolin clay has been previously used as a model for the flocculation of polyelectrolytes.[5] To understand the behavior of organic charged particles undergoing flocculation in the presence of charged polymers, it would be interesting to study a polymeric system in the presence of charged micelles.

Following a study performed on noncharged polymers, i.e., the NMR study of the interaction between poly(vinylpyrrolidone) and charged fluorinated micelles,[7−9] a similar approach was attempted on a charged copolymer (acrylamide−trimethylaminoethyl acrylate). In this paper, because of the industrial interest in charged copolymers, the influence of a different charge density in the interaction with an oppositely charged surfactant was tested, using copolymers purposely synthesized. According to the usual approach reported in the literature,[10] all measurements were performed using a constant concentration of polymer and increasing amounts of surfactant. In this way it was possible to not only study the flocculation mechanism and the optimal flocculation concentration (OFC) but also obtain a molecular description of those mechanisms of polymer−surfactant interaction causing the flocculation process.

Two mechanisms of flocculation have been proposed, the so-called polymer bridging and the electrostatic patch attraction.[5,6] The aim of this study is to make a clear distinction of these effects. Furthermore, studying samples at concentrations above the cmc, useful information can be obtained regarding the direct complexation between charged polymers and charged micelles. Consequently, precise direct information can be gathered about possible polymer bridge among different micelles. Like most physical−chemical studies,[10−12] NMR spectroscopy shows that there is a strong interaction between charged polymers and micelles leading to the formation of a complex. A subtler effect, i.e., the modulation of the kinetics of exchange between free and bound micelles by charge density and surfactant concentration, can be better observed and studied using the NMR approach.

## Experimental Section

**Materials.** All monomers, 2-(dimethylamino)ethyl methacrylate methyl chloride quaternary salt (DMAEA) and acrylamide (AAm), were obtained by Aldrich. AAm was freshly distilled before use. DMAEA was purified by repeated extraction with acetone: the powder obtained was then dried in a vacuum oven and stored in a freezer. The initiator *N,N*-azobis(isobutyronitrile) (AIBN) was purchased by Aldrich and purified by crystallization.

† Istituto di Metodologie Chimiche.
‡ Università degli Studi di Catania.
§ Università degli Studi di Roma "La Sapienza".
* To whom correspondence should be addressed.

10.1021/ma012238t CCC: $22.00 
Published on Web 04/18/2002

**Table 1. Polyelectrolyte Characteristics: Viscosity-Average Molecular Weights, $M_v$, of Poly(acrylamide−trimethylaminoethyl acrylate), $C$, Concentration Where Maximum of $^1$H Line Width Is Observed, $\bar{C}$, Concentration Corresponding to Middle Precipitation Range**

| charge density (%) | $M_v$ (dL/g) | $C$ (mM) | $\bar{C}$ (mM) |
|---|---|---|---|
| 14 | $1.51 \times 10^4$ | 10.3 | ∼8 |
| 23 | $1.58 \times 10^4$ | 18.0 | ∼15 |
| 42 | $1.72 \times 10^4$ | 35.8 | ∼40 |
| 54 | $2.00 \times 10^4$ | 41.6 | ∼50 |

**Table 2. Poly(acrylamide−trimethylaminoethyl acrylate): $^1$H and $^{13}$C Chemical Shifts (ppm) Assignment**

| P(AAm) | P(TAMEA) |
|---|---|
| $C_\alpha \sim 42$; $H_\alpha \sim 2.2$ | $C_\alpha \sim 41$; $H_\alpha \sim 2.5$ |
| $C_\beta \sim 35$; $H_\beta \sim 1.7$ | $C_\beta \sim 35$; $H_\beta \sim 1.8$ |
| $C_{1'} = 177$ | $C_1 = 180$ |
| | $C_2 = 59$; $H_2 = 4.6$ |
| | $C_3 = 65$; $H_3 = 3.8$ |
| | $C_4 = 54$; $H_4 = 3.2$ |

**Table 3. $^{19}$F Chemical Shifts (ppm) Assignment for Lithium Perfluorooctanoate (0.68 mM): $^8CF_3-^7CF_2-^6CF_2-^5CF_2-^4CF_2-^3CF_2-^2CF_2-^1COOLi$**

| atom | $^{19}$F (ppm) | atom | $^{19}$F (ppm) |
|---|---|---|---|
| C-2 | −39.60 | C-6 | −44.90 |
| C-3 | −45.37 | C-7 | −48.20 |
| C-4 | −43.95 | C-8 | −2.94 |
| C-5 | −44.18 | | |

Polymerizations were performed under dry argon using standard Schlenk techniques. All glassware was oven-dried overnight at 175 °C before use and flamed after assembling.

In a typical synthesis DMAEA (0.013 mol), AAm (0.011 mol), and AIBN (0.02 g) were dissolved in 50 mL of water/ethanol (5/5 v/v). The mixture was degassed by repeated freeze−thaw cycles. Polymerizations were performed at 75 °C overnight. The reactions were stopped by cooling, and the polymers were isolated by repeated precipitations in an acetone:methanol (90:10) mixture.

By changing the DMAEA/AAm ratio, we obtained four polymers having different charge densities, defined as the molar ratio between DMAEA and the total amount of DMAEA and AAm incorporated in the polymer. Charge densities, estimated by $^1$H NMR experiments from the ratio of the integrated intensities of α- and β-protons of the alkyl side chains to the peak corresponding to the polymers backbone protons, were established as being 14, 23, 42, and 54%. Absence of monomer was checked by $^1$H NMR spectroscopy. Lithium perfluorooctanoate, LiPFO, was prepared by dissolving perfluorooctanoic acid (Aldrich) in ethanol and neutralizing with lithium hydroxide in aqueous solution. The end point of titration was established using phenolphthalein as an indicator. The alcohol was removed by heating, and the solution was freeze-dried.

Surfactant, polymer, and polymer−surfactant solutions were prepared in deuterium oxide (Isotec. Inc., 99.9% purity).

**Viscosity Measurements.** The viscosity-average molecular weights, $M_v$, of the polymers were estimated by capillary viscometry in 1 M NaCl solutions at 25 °C. The Mark−Houwink parameters were $k = 1.05 \times 10^4$ dL/g and $\alpha = 0.73$.[17] The molecular weights of polyelectrolytes are reported in Table 1.

**NMR Experiments.** $^1$H spectra were run either on a Varian Unity INOVA 500 operating at 499.88 MHz or on a Bruker AMX 600 spectrometer at 600.13 MHz. All $^{19}$F NMR spectra were run on a Varian Unity INOVA 500 operating at 470.302 MHz. $^1$H chemical shifts are given in ppm with respect to external TMS (tetramethylsilane). $^{19}$F NMR chemical shifts are given in ppm with respect to external $CF_3COOH$ assumed to be at 0.0 ppm. Assignment of $^{19}$F resonances was previously reported.[13] $^{13}$C spectra were run on a Bruker AMX 600 operating at 150.91 MHz and referred to external TMS. Full spectra assignment was obtained by a series of 1D and 2D experiments (COSY,[14] TOCSY,[15] HMQC[16]) performed with a gradient selection and reverse detection. $^1$H and $^{13}$C spectra assignments, concerning polyelectrolytes, are reported in Table 2.

$^{19}$F spectra assignment, concerning the surfactant, are reported in Table 3.

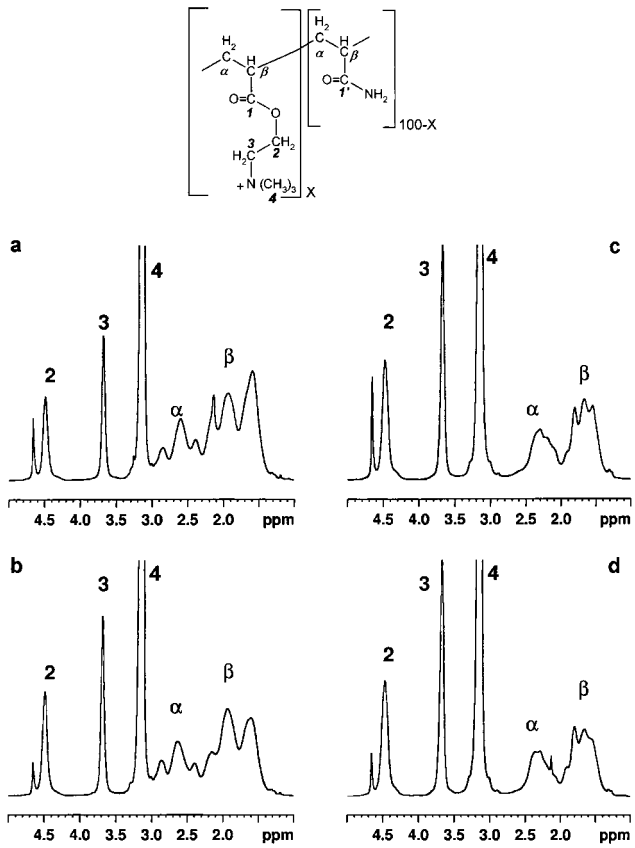


**Figure 1.** $^1$H NMR resonances of P(AAm−TMA), $D_2O$ solution (1% w/w): (a) charge density 14%, (b) charge density 23%, (c) charge density 42%, (d) charge density 54%.

## Results and Discussion

**$^1$H NMR Spectroscopy.** The $^1$H NMR spectra of the polyelectrolyte P(AAm−TMA) are shown in parts a, b, c, and d of Figure 1 where the charge density is 14%, 23%, 42%, and 54%, respectively. Full assignment of the spectra is reported in the same figure. $^1$H spectra of 14% and 23% polymers show a much higher multiplicity than the corresponding spectra of polymers with a charge density of 42% and 54% (see Figure 1). In accordance with literature data[18,19] at low charge density the polyelectrolyte presents a flexible coil structure in which many different conformers are present. On the contrary, at high charge density a stiff rodlike structure is present. The above interpretation is consistent with $^{13}$C spectra (see Figure 2), where the number of resonances present in the spectra of high charged polymers is much lower than that of the low charged polymers.

The addition of LiPFO up to a concentration $C$ causes only small changes in the $^1$H spectra. In fact, in all samples where the amount of the surfactant is increased up to a critical value, no broadening occurs. However, in correspondence of a $C$ value, dependent on the charge density of the polymer, a marked broadening of all $^1$H NMR resonance lines is detectable (see for instance Figures 3 and 4). The particular concentration $C$ where the maximum of $^1$H line width is visible is reported in

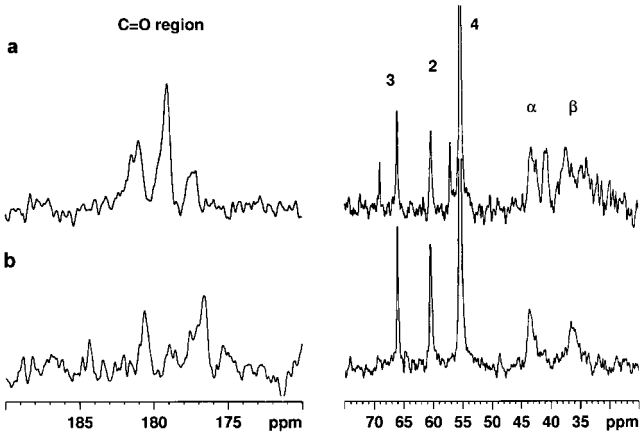


**Figure 2.** $^{13}C$ NMR resonances of P(AAm−TMA), $D_2O$ solution (1% w/w): (a) charge density 14%, (b) charge density 54%.

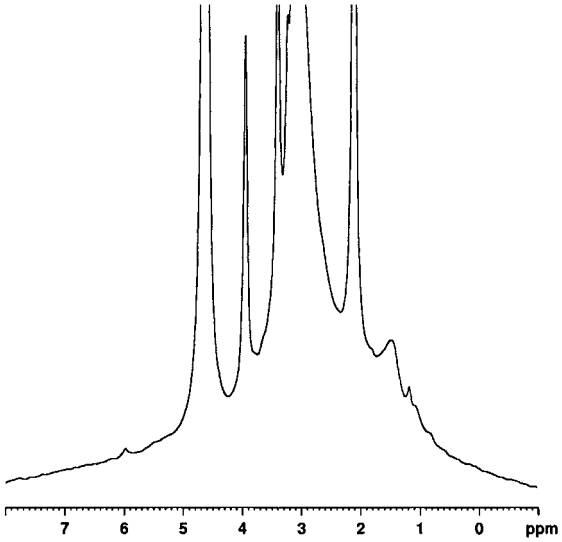


**Figure 3.** $^1H$ NMR resonances of P(AAm−TMA) at 14% charge density, in the presence of LiPFO; molal concentration $m = 10$ mM.

Table 1, column 3. Note that all polyelectrolytes have comparable molecular weight; therefore, any line broadening observed in the NMR spectra cannot be attributed to the molecular weight of polymers. This critical concentration value *C* may be interpreted as being due to the so-called "cac", i.e., the concentration of critical aggregation.

The strong interaction between a charged surfactant and an opposite charged polyelectrolyte causes precipitation at particular surfactant concentrations. This observation is in accordance with previously reported literature data.[20−24] In the same table, see the last column, the approximate center of the precipitation range, *C*, is reported. At low concentrations of added surfactant, the polymer solutions show a noticeable increase of turbidity and subsequently a precipitate, with the maximum precipitation corresponding to a charge neutralization. The addition of an excess surfactant results in the complete clarification of the solution as the complex is resolubilized. Recently, this process has been monitored using many experimental techniques such as light scattering[25] and turbidimetry.[26,27] $^1H$ NMR measurements can be used to monitor the precipitation process associated with the complexation phenomena.

Note that, even in the presence of a "precipitate", an $^1H$ NMR spectrum can be seen. This spectrum shows a

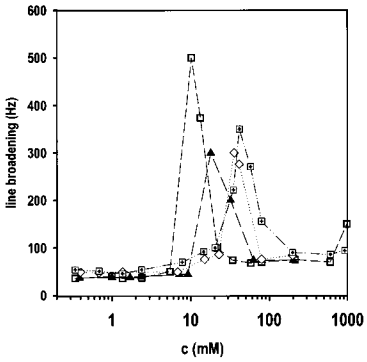


**Figure 4.** Line width of the $^1H$ resonances of $O-CH_2$ as a function of the surfactant concentration in $D_2O$: LiPFO−P(AAm−TMA) 14% (□), LiPFO−P(AAm−TMA) 23% (▲), LiPFO−P(AAm−TMA) 42% (◊), LiPFO−P(AAm−TMA) 54% (⊡). The actual value of the maximum depends strongly on the concentration and is poorly defined. No importance must be given to the line broadening value, when larger than ≈300 Hz.

broad super-Lorentzian line[28−30] surmounted by a spectrum in which some chemical shifts are still visible. The maximum broadening of the super-Lorentzian line is exactly halfway through of the precipitation range (see the last two columns of Table 1).

Therefore, the $^1H$ spectrum of the so-called "precipitate" is still detectable, meaning that some residual mobility of the system polyelectrolyte−LiPFO is still present; i.e., we are in the presence of the so-called "soft matter" and not of a true solid which should give too broad an $^1H$ NMR line to be visible. The presence of sharp lines means that in the range where precipitation takes place part of the polymer and part of the surfactant are still in solution. The total integral of the fraction of the sharp $^1H$ NMR signal is reported as a function of surfactant concentration. This is a measurement of the residual concentration of the polymer in solution (see Figure 5). Consequently, even if $^1H$ NMR data are poorly defined, nevertheless three concentration ranges are evident. In the first one the interaction is merely an electrostatic coupling of surfactant molecules and cationic sites. At a much higher surfactant concentration, the third range, the bridging mechanism involving the micelles and the polymeric chain, is the dominat one. These two ranges are separated by a "precipitation" range whose onset is clearly lowered at low charge density. The precipitation range as a whole is modulated by the absolute concentration of the polymeric moiety and by its charge density.

**$^{19}F$ NMR Spectroscopy.** Chemical shift values and the relative assignment of LiPFO in water, concentration 0.68 mM, are given in Table 3.

The dependence of $^{19}F$ chemical shift on the surfactant concentration is shown in Figure 6 for the resonances due to fluorine atoms in position 7. At lower concentrations a flat trend is noticeable, followed in correspondence with the cmc by a sudden downfield shift at higher concentrations; this plot exhibits a feature typical of most amphiphilic compounds.[31−34] The value of cmc found by $^{19}F$ NMR is in accordance with the values obtained by other techniques.[35]

The micellization process can be also observed using the variation of the line width as a function of the surfactant concentration. In fact above the cmc, the $^{19}F$ NMR lines of LiPFO show only a slight broadening clearly visible on all resonances. The broadening observed can be interpreted as a fast exchange between a

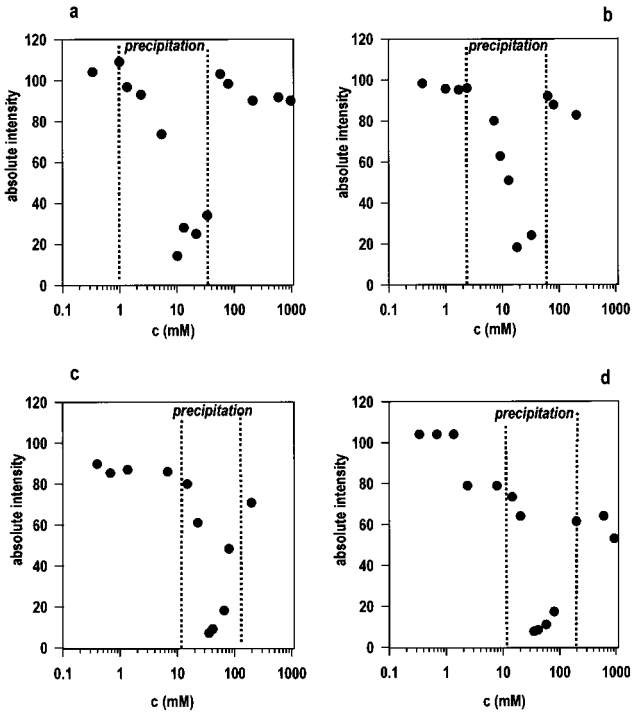


**Figure 5.** Intensity of the sharp $^1$H NMR resonances as a function of the surfactant concentration: (a) P(AAm−TMA) 14%; (b) P(AAm−TMA) 23%; (c) P(AAm−TMA) 42%; (d) P(AAm−TMA) 54%. Precipitation range are shown by dotted lines. The resonance intensities are expressed as percentages of integrated peak areas normalized with respect to their values in the absence of surfactant. The $^1$H spin density does not change in the whole concentration range.

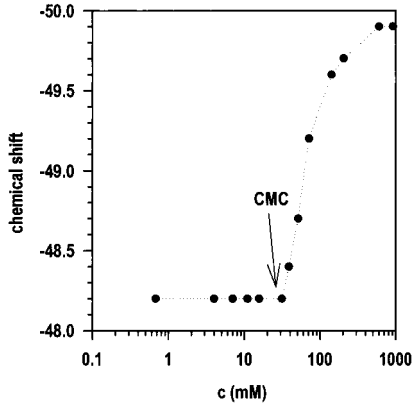


**Figure 6.** $^{19}$F chemical shift for fluorine atoms bound to C7 against logarithm of surfactant concentration.

sharp resonance (<10 Hz) due to the monomeric moiety and a slightly broader resonance (≈30 Hz) due to the micelles.

In the presence of the polyelectrolyte P(AAm−TMA), a marked broadening of all the $^{19}$F NMR resonances of the surfactant occurs. This loss of resolution causes some signal overlap, namely those due to fluorine atoms in positions 3, 4, 5, and 6. Therefore, only the behavior of the resonances due to fluorine atoms in positions 2, 7, and 8 will be discussed.

In Figure 7a, the dependence of $^{19}$F chemical shifts on the surfactant concentration of fluorine atoms in position 2 for the LiPFO−polyelectrolyte systems is reported and compared with that of the LiPFO system alone.

At very low surfactant concentration (0.1−1mM) a marked downfield variation, 0.4−0.6 ppm, is visible for

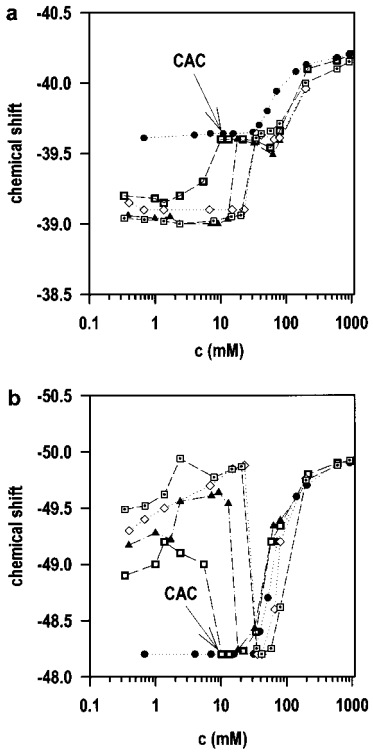


**Figure 7.** (a) Chemical shift for fluorine atoms bound to C2 against logarithm of surfactant concentration. (b) Chemical shift for fluorine atoms bound to C7 against logarithm of surfactant concentration. LiPFO system (●), LiPFO−P(AAm−TMA) 14% (□), LiPFO−P(AAm−TMA) 23% (▲), LiPFO−P(AAm−TMA) 42% (◊), LiPFO−P(AAm−TMA) 54% (⊡).

the $CF_2$(2) resonance with respect to the LiPFO system, showing a full complexation of LiPFO with all polyelectrolytes. At this concentration range the molecules of LiPFO are in a monomeric state, and a dynamic equilibrium exists between the monomer and a complex formed by LiPFO bound to the charged sites of the polyelectrolyte.

Increasing the surfactant concentration (1−30 mM), the behavior of the resonances due to $CF_2$(2) depends on the charge density of the polyelectrolyte. In fact, the first variation in the chemical shift trend is visible for the polyelectrolyte with a 14% charge density. In this system when a precipitation takes place, the chemical shift values of resonances due to $CF_2$(2) approach the value observed in the LiPFO system; when the polymer has completely precipitated, the chemical shift values are exactly the same as in the LiPFO system. Therefore, the few molecules still present in the solution are due to the free surfactant alone.

In the same concentration range, the behavior of polyelectrolytes at a higher charge density is quite similar to that seen in the 14% polyelectrolyte; the main difference is the concentration at which the chemical shift values move upfield toward those of the LiPFO system. In fact, this concentration mainly depends on the saturation of the charged sites of the polymer: the higher the charge density, the greater the concentration where chemical shift values approach the trend of the LiPFO−water system.

In accordance with previously reported data[36,37] in the presence of polyelectrolytes P(AAm−TMA), the critical micellar concentration of the surfactant is delayed; i.e., a postposition of the cmc value is noticeable. However, the value of the cac observed in Figure 7 is more interesting. In accordance with the $^1$H data, the onset

of precipitation anticipates in both low charge density polymers and retards in both the high-density polymers.

Regarding the trend of chemical shift values of $CF_2$-(7), Figure 7b shows that the presence of polyelectrolytes leads to an upfield variation of about 1−1.5 ppm. The variation of the chemical shift depends on the charge density of the polyelectrolytes even at the initial range. Since the chemical shift in question is of a group far from the polar head, a full complexation of the monomer with the charged polymer occurs, which modifies the chemical environment of the hydrophobic end of the monomer. Increasing the surfactant concentration, near the precipitation range of the systems, a downfield trend of chemical shifts values is detectable approaching the values of the LiPFO system. Depending on the charge density, in the whole concentration range before precipitation, a full differentiation of chemical shifts of $CF_2$(7) group takes place. Note that, when the polymer has completely precipitated, the chemical shift value of $CF_2$(7) group returns to that of the LiPFO system. In proximity of the critical micellar concentration the values of $CF_2$(7) chemical shifts indicate a postposition of the cmc.

The behavior of the chemical shift of the resonance due to $CF_2$(7) is completely different from that of resonances due to $CF_2$(2). The peculiar behavior of the $CF_2$(2) resonance can be attributed to the nearby charge neutralized during the complexation.[38]

It is worth noting that in both cases (fluorine atoms bound to C2 and to C7) the presence of the polyelectrolyte influences mainly the chemical shift trend in the premicellar region rather than that of the postmicellar region. This phenomenon can be attributed to the different environment around the alkyl fluorinated chains. Before micellization the fluorinated chains are exposed to the interaction with the polyelectrolyte that deeply affects the chemical shifts; after micellization the fluorinated chain are inside the micelle core. In this situation, the polyelectrolyte interacts with micelles in a so-called "bridging" interaction that affects mainly the polar heads of the surfactant.

Finally, the chemical shifts of the $CF_3$ group are considered as a function of the surfactant concentration for all systems LiPFO−polyelectrolyte and also for LiPFO (see Figure 8).

As observed for $CF_2$(7) resonances, in the presence of polyelectrolytes the chemical shift values of the $CF_3$ group undergo an upfield shift even at a very low surfactant concentration (0.1−1 mM). Increasing the LiPFO concentration and reaching the precipitation range a downfield variation of the chemical shift of $CF_3$ is visible. The concentration where such variation occurs depends on the charge density of the system. Besides the $CF_3$ group shows a particular behavior: in fact, in the range where precipitation of the polyelectrolytes−surfactant systems takes place, a splitting of the $CF_3$ resonance is observed (see Figure 8, gray symbols). In view of the above consideration, the splitting of $CF_3$ resonances can be attributed to the equilibrium that exists between the free surfactant and the bound polymer surfactant assuming that this equilibrium occurs with an exchange rate slower than the NMR observation time. After redissolution of the system the behavior of the chemical shift is quite similar to that observed for the fluorine atoms bound to C7. In this case the postposition of the cmc of the LiPFO is clearly evident for the polyelectrolytes with the greater charge density.

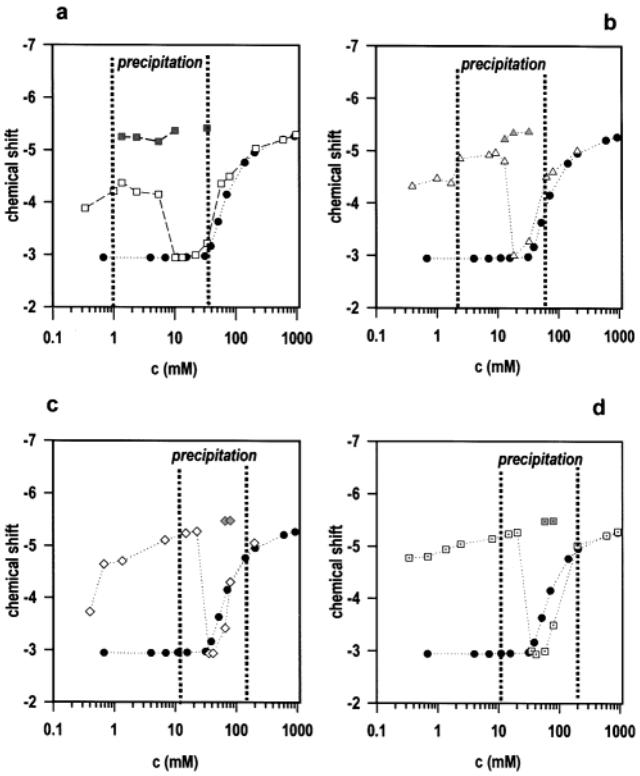


**Figure 8.** Chemical shift for fluorine atoms bound to C8 against logarithm of surfactant concentration. LiPFO system (●), LiPFO−P(AAm−TMA) 14% (□), LiPFO−P(AAm−TMA) 23% (□), LiPFO−P(AAm−TMA) 42% (◊), LiPFO−P(AAm−TMA) 54% (⊡). Precipitation range are shown by dotted lines.

Now only the behavior of the line widths of $^{19}F$ resonances remains to be considered.

As is well-known,[39] the shape and the width of nuclear magnetic resonances are sensitive to a time-dependent process which occurs at rates of the order of NMR time observation. It is approximately assumed the exchange rate constant at the equilibrium between two forms depends on the temperature, the potential barrier $E_a$, and the frequency of NMR resonances, as shown in eq 1:

$$\log \frac{1}{2\pi\tau(\nu_a - \nu_b)} = \log \frac{k_0}{\pi(\nu_a - \nu_b)} - \frac{E_a}{2.3RT} \qquad (1)$$

In the approximation of equimolar components and supposing that chemical shift values are not a function of the concentration,[40] it is possible to observe three cases with different rate constants:

case a: $2\pi\tau(\nu_a - \nu_b) \geq 2$

$\tau =$ S

(slow with respect to NMR observation time)

case b: $\sqrt{2} < 2\pi\tau(\nu_a - \nu_b) \leq 1$

$\tau =$ s (similar to NMR observation time)

case c: $2\pi\tau(\nu_a - \nu_b) < 0.5$

$\tau =$ F

(fast with respect to NMR observation time)

In the case of large $\tau$ two lines at $\nu_a$ and $\nu_b$ are clearly visible, whereas for small $\tau$ only one line halfway between both is given.

Therefore, if a dynamic equilibrium among two forms occurs with an exchange rate faster than the NMR observation time, a single sharp line is visible; if the exchange at the equilibrium is slow, two distinct lines are detectable, whereas one single very broad line is present in the intermediate case.

To understand and rationalize the line widths observed on $^{19}F$ NMR lines, it is useful to note that micelles bound to a charged polymer constitute the stiffest possible system, i.e., the system with the shortest $T_2$ value.[9] However, the enlargement of an NMR line is not necessarily due to a molecular stiffness; in fact, very broad lines can be seen when an exchange between two or more forms occur in a time comparable to the NMR observation time.[41] Therefore, the simple observation of an enlargement of an NMR line usually indicates the presence of two or more chemical entities in a slow exchange.

Then from the analysis of line widths the order of magnitude of the rate constant for the interchange can be deduced as

$$\begin{array}{ccc} \text{[LiPFO monomeric]} & \leftrightarrows & \text{[monomeric LiPFO - charged polymer]} \\ \updownarrow & & \updownarrow \\ \text{[LiPFO micelles]} & \leftrightarrows & \text{[micelles of LiPFO - charged polymer]} \end{array}$$

This behavior is confirmed by the analysis of the peak width of $CF_2(2)$ and $CF_2(7)$ groups (see Figure 9a,b). In the presence of polylelectrolytes, at a very low surfactant concentration (0.1−1 mM), the line width is very different compared to the line width obtained for a binary system. This result confirms that a dynamic equilibrium exists between a free LiPFO monomer and a LiPFO bound to the charged site of the polyelectrolyte and that the exchange rate of this equilibrium occurs in a time observable using the NMR technique.

In Figure 9 it is possible to observe a strong charge density effect on the line widths of the resonances of $CF_2(2)$ and $CF_2(7)$; that is, the stronger the charge density, the faster the equilibrium between free molecules of the surfactant and the complex. This observation is in complete accordance with the kinetic theory in solution; it is known that a reaction speed up at increasing concentration. Above the cmc, after polyelectrolyte saturation, the line width of $CF_2(2)$ and $CF_2(7)$ becomes quite similar to that of the LiPFO system. In this concentration range the free micelles become the dominant species in solution, and the line width observed in the presence of polyelectrolytes is approximately of the same magnitude as the broad resonance detectable in unbound micelles (≈30 Hz).

More kinetic information is contained in the shape of the $CF_3$ resonance (see Figure 10). Here (see Figure 10a), at a low charge density and at a concentration of about 1 mM, the exchange between species [bound] ⇆ [unbound] is so slow that it is possible to see two resonance lines, i.e., case a. Increasing the charge density, case a is reached only at a higher surfactant concentration, namely 10 mM for 23% (Figure 10b), 60 mM for 42% and 54% (see Figure 10c,d).

It is worth noticing that the line widths visible for the $CF_3$ group are smaller than those of other resonance lines. In fact, $CF_3$ groups originate rather sharp lines due to their intrinsic mobility.

Finally, as already seen in $^1H$ NMR spectra, also $^{19}F$ NMR spectra show a general loss of intensity of all resonance lines when precipitation occurs, meaning that the polymer precipitates carry only a part of LiPFO. At a higher surfactant concentration, after the resolubilization, a super-Lorentzian $^{19}F$ line is detectable super-

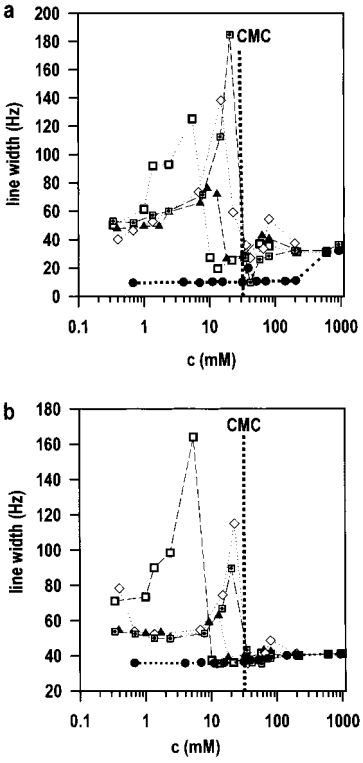


**Figure 9.** (a) Line width of the $^{19}F$ resonances of $CF_2(2)$ as a function of the surfactant concentration in $D_2O$. (b) Line width of the $^{19}F$ resonances of $CF_2(7)$ as a function of the surfactant concentration in $D_2O$. LiPFO system (●), LiPFO−P(AAm−TMA) 14% (□), LiPFO−P(AAm−TMA) 23% (▲), LiPFO−P(AAm−TMA) 42% (◊), LiPFO−P(AAm−TMA) 54% (⊡). The cmc value is shown by a dotted line.

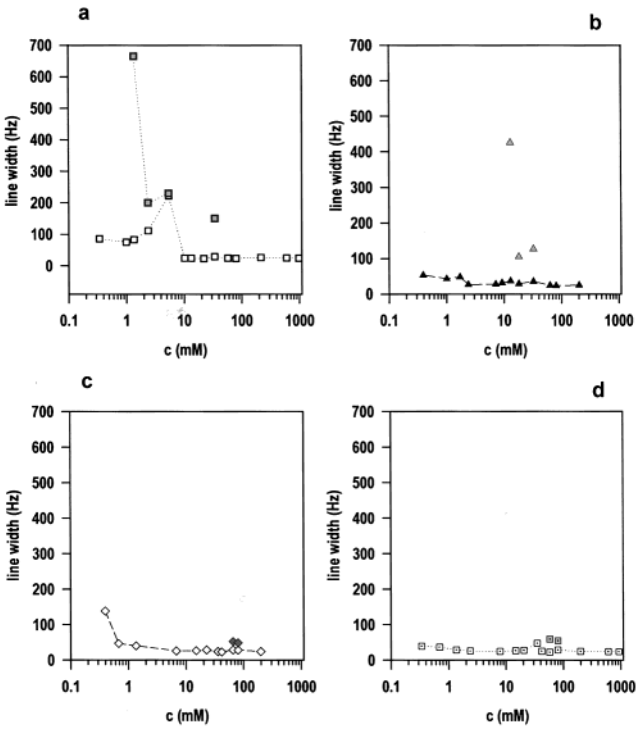


**Figure 10.** Line width of the $^{19}F$ resonances of $CF_3$ as a function of the surfactant concentration in $D_2O$. LiPFO system (●), LiPFO−P(AAm−TMA) 14% (□), LiPFO−P(AAm−TMA) 23% (▲), LiPFO−P(AAm−TMA) 42% (◊), LiPFO−P(AAm−TMA) 54% (⊡).

imposed again by a sharp spectrum. The presence of the super-Lorentzian $^{19}F$ line can be interpreted as an indicator of the incoming gelification of the mixture.

## Conclusions

It has been shown that $^{1}H$ NMR and $^{19}F$ NMR spectroscopies can provide molecular-level details regarding the nature and degree of electrostatic interaction between a polyelectrolyte and an oppositely charged fluorinated surfactant. Experimental evidence suggests that the process leading to polymer−surfactant aggregates is a multistage complex mechanism. The association between the polyelectrolyte and the surfactant starts at the very low concentration range and strongly depends on the charge density of the polyelectrolyte.

Note that, as a function of the charge density, the whole structure of the polyelectrolyte changes. In fact, increasing the charge density, the overall shape of the macromolecule in solution turns from a flexible coil into a rigid-rod-like structure.

At a low surfactant concentration, the interaction of the surfactant molecules with the polymer is mostly driven by the strong electrostatic attraction between the opposite charges. Other driving forces acting in this association are the hydrophobic interactions between surfactant tails and the polymer backbone, which is hydrophobic. Increasing the surfactant concentration $^{1}H$ NMR spectra show marked line broadening, occurring at a well-defined critical surfactant concentration, *C***.** This concentration has been interpreted as cac; its value markedly increases at an increasing charge density of polyelectrolytes.

The strong surfactant−polyelectrolyte interaction leads to the precipitation phenomenon that becomes almost complete when a full charge neutralization is reached. The precipitation range shifts at higher surfactant concentrations at increasing charge density of the polymer.

In the same concentration range, changes in the $^{19}F$ chemical shift of the surfactant are observed. A strong kinetic effect is observable. In fact, the line widths of $^{19}F$ resonances show the presence of a dynamic equilibrium between free micelles and micelles bound to the polyelectrolyte. This behavior is modulated by the polymer charge density, and it is sensitive to the surfactant concentration.

Increasing the surfactant concentration, the LiPFO monomers bound to the macromolecule form "nuclei" for further binding of micelles. Consequently, the polyelectrolyte resolubilizes, being stabilized in solution by interactions with the charged micelle surface.

At a very high surfactant concentration numerous chains of polyelectrolyte are able to perform complexation with many charged micelles.

Note that polylelectrolytes with a 14% and 23% charge density show a cac value lower than the cmc of the surfactant. On the contrary, polyelectrolytes with the higher charge density of 42% and 54% show very similar cac and cmc values. As a consequence, values too high in charge density can give effects unfavorable in the industrial process where flocculation of colloidal particles is required. In the wastewater treatments, for example, the role of the polyelectrolyte is to promote the flocculation process at a very low concentration of colloidal compounds. Our results on polymers at a charge density of 42% and 54% reveal that an excessive charge of polyelectrolytes may be unfavorable in the whole industrial process, delaying the beginning of flocculation and indicating a postposition of the precipitation range.

NMR methods would appear extremely useful in revealing the best range of charge density to be used for each specific problem both as regards the flocculation phenomena as well as clarifying the interactions between macromolecular charged systems.

## References and Notes


(1) Svarovsky, L. In *Solid-Liquid Separation*; Butterworth: London, 1990.
(2) Moudgil, B. M.; Somasundaran, P. *Colloids Surf.* **1985**, *13*, 87.
(3) Villar, J. W.; Dawe, G. A. *Min. Congr. J.* **1975**, *61*, 40.
(4) Somasundaran, P.; Cleverdon, J. *Colloids Surf.* **1985**, *13*, 73.
(5) Chen, J. *Sep. Sci. Technol.* **1988**, *33*, 569.
(6) Everett, D. H. In *Basic Principles of Colloid Science*; Royal Society of Chemistry: London, 1988.
(7) Sesta, B.; Segre, A. L.; D'Aprano, A.; Proietti, N. *J. Phys. Chem. B* **1997**, *101*, 198.
(8) Sesta, B.; D'Aprano, A.; Segre, A. L.; Proietti, N. *Langmuir* **1997**, *13*, 6612.
(9) Segre, A. L.; Proietti, N.; Sesta, B.; D'Aprano, A.; Amato, M. E. *J. Phys. Chem. B* **1998**, *102*, 10248.
(10) Goddard, E. D. In *Interaction of Surfactant with Polymers and Proteins*; Goddard, E. D., Ananthapadmanabhan, K. P., Eds.; CRC Press: Boca Raton, FL, 1993.
(11) Ohbu, K.; Hiraishi, O.; Kashiwa, I. *J Am. Oil Chem. Soc.* **1982**, *59*, 108.
(12) Dubin, P. L.; Oteri, R. *J. Colloid Interface Sci.* **1983**, *95*, 453.
(13) Amato, M. E.; Caponetti, E.; Chillura Martino, D.; Pedone, L. *J. Phys. Chem. B*, in press.
(14) Braun, S.; Kalinowsky, H. O.; Berger, S. In *100 and More Basic NMR Experiments*; VCH Publisher: Weinheim, Germany, 1996.
(15) Kövér, K. E.; Uhrin, D.; Hruby, V. J. *J. Magn. Reson.* **1998**, *130*, 162.
(16) Hurd, R. E.; John, B. K. *J. Magn. Reson.* **1991**, *91*, 648.
(17) Mabire, F.; Audebert, R.; Quivoron, C. *Polymer* **1984**, *25*, 1317.
(18) Doi, M.; Edwards, S. F. In *The Theory of Polymer Dynamics;* Oxford University Press: New York, 1986; p 2.
(19) Garces, F. O.; Sivadasan, K.; Somasundaran, P.; Turro, N. J. *Macromolecules* **1994**, *27*, 272.
(20) Goddard, E. D.; Hannan, R. B. *J. Colloid Interface Sci.* **1976**, *55*, 73.
(21) Leung, P. S.; Goddard, E. D.; Han, C.; Glinka, C. J. *Colloids Surf.* **1985**, *13*, 47.
(22) Goddard, E. D.; Leung, P. S. *Polym. Prepr. (Am. Chem. Soc., Div. Polym. Chem.)* **1982**, *23*, 47.
(23) Goddard, E. D.; Hannan, R. B. In *Micellization, Solubilization and Microemulsion;* Mittal, K. L., Ed.; Plenum Press: New York, 1977; Vol. 2, p 835.
(24) Lindmann, B.; Holmberg, K.; Kronberg, B. In *Surfactants and Polymers in Aqueous Solution*; John Wiley & Sons Ltd.: Chichester, 1998; pp 236−240.
(25) Dubin, P.; Thé, S.; McQuigg, D.; Gan, L.-M. *Langmuir* **1990**, *6*, 1422.
(26) Dubin, P.; Oteri, R. *J. Colloid Interface Sci.* **1983**, *95*, 453.
(27) Dubin, P.; Rigsbee, D.; Gan, L.-M. *Macromolecules* **1988**, *21*, 2555.
(28) Morrison, C.; Henkelman, R. M. *Magn. Reson. Med.* **1995**, *33*, 475.
(29) Quesson, B.; Thiaudiere, E.; Delalande, C.; Dousset, V.; Chateil, J.-F.; Canioni, P. *Magn. Reson. Med.* **1997**, *38*, 974.
(30) Capitani, D.; Casieri, C.; Briganti, G.; La Mesa, C.; Segre, A. L. *J. Phys. Chem. B* **1999**, *103*, 6088.
(31) Wennerstrom, H.; Lindmann, B.; Soderman, O.; Drakenbert, T.; Rosenholm, J. *J. Am. Chem. Soc.* **1979**, *101*, 6860.
(32) Drakenbert, T.; Lindmann, B. *J. Colloid Interface Sci.* **1973**, *44*, 184.
(33) Soderman, O.; Lindmann, B.; Stilbs, P. In *Nuclear Magnetic Resonances*; Webb, G. A., Ed.; Chemical Society, London, 1983; Vol. 12, p 302.
(34) Soderman, O. In *Nuclear Magnetic Resonances*; Webb, G. A., Ed.; Chemical Society, London, 1983; Vol. 14, p 350.

(35) Muzzalupo, R.; Ranieri, G. A.; La Mesa, C. *Colloids Surf. A* **1995**, *104*, 327.
(36) Cabane, B.; Duplessix, R. *J. Phys. (Paris)* **1982**, *43*, 1529.
(37) Lindmann, B.; Holmberg, K.; Kronberg, B. In *Surfactants and Polymers in Aqueous Solution*; John Wiley & Sons Ltd: Chichester, 1998; pp 220−222.
(38) Saika, A.; Slichter, C. P. *J. Phys. Chem.* **1954**, *26*, 968.
(39) Pople, J. A.; Schneider, W. G.; Bernstein, H. J.; Schneider, W. G.; Bernstein, H. J. In *High-Resolution Nuclear Magnetic Resonance*; McGraw-Hill Book Co.: New York, 1959; p 367.
(40) Pople, J. A.; Schneider, W. G.; Bernstein, H. J.; Schneider, W. G.; Bernstein, H. J. In *High-Resolution Nuclear Magnetic Resonance*; McGraw-Hill Book Co.: New York, 1959; pp 223−225.
(41) Pople, J. A.; Schneider, W. G.; Bernstein, H. J.; Schneider, W. G.; Bernstein, H. J. In *High-Resolution Nuclear Magnetic Resonance*; McGraw-Hill Book Co.: New York, 1959; pp 218−220.

MA012238T